Experimentally Validated Bounding Models for the Scout II Quadrupedal Robot

Ioannis Poulakakis and James A. Smith
Centre for Intelligent Machines, McGill University
Montreal, H3A 2A7, Canada
{poulakas & jasmith}@cim.mcgill.ca

Martin Buehler[1]
Boston Dynamics
Cambridge, MA 02139, USA
buehler@BostonDynamics.com

Abstract **- In this paper the authors discuss control and modeling issues significant for constructing simple running controllers and building experimentally validated simulation models for dynamically stable robots. A bounding controller resulting in dynamically stable running up to 1.3 m/s for the Scout II quadruped is presented. Simulation models are built and compared with experimental data to test the viability of various simplifying assumptions common in the literature for running robots. The authors demonstrate the need for including motor saturation and nonrigid torque transmission characteristics into simulation models. Similar issues are likely to be important in other legged robots as well. An extensive suite of experimental results documents the robot's performance and validates simulation models.**

Index Terms **- Legged robots, bounding gait, dynamic running, model validation, quadrupedal robot.**

I. Introduction

As more robots are designed to operate in the real world the limitations of traditional wheeled and tracked vehicular designs have become increasingly apparent. To overcome these limitations one branch of the mobile robotics field has turned to biological inspiration for other possible solutions including legged systems, which promise a versatility and mobility unparalleled in more traditional designs.

Early attempts to implement legged designs resulted in slow moving statically stable systems; these designs are still the most prevalent today. However, in this paper we restrict our attention to dynamically stable legged robots. To date, the most significant research on dynamic legged locomotion occurred at the MIT Leg Lab in the 1980s and 1990s, [12]. Raibert's research revolved around simple fundamental principles for controlling hopping height, forward speed and body posture, making complex gaits possible on monopedal, bipedal and quadrupedal robots. His controllers, although very simple, resulted in high performance running with different gaits. Our recent research showed that even simpler control laws, just positioning the legs at a desired touchdown angle, *without* requiring task-level or torso-state feedback, can achieve stable running at speeds up to 1.3 m/s in Scout II (Fig.1), despite the absence of active control over leg length, and with only one actuator per leg, [14].

Other dynamically stable designs have been proposed since Raibert, including the implementation of a bounding gait in the Scamper quadruped by Furusho et al. [4]. Even though the robot's legs were not designed with explicit mechanical compliance, the compliance of the feet, legs, belt transmissions, and the PD joint servo loops were likely significant. The controller divided one running cycle into eight states and switched the two joints per leg between free rotation, position control and velocity control. Kimura et al. implemented a bounding gait in the Patrush robot using a neural oscillator based controller, [5]. Each three degree of freedom (DOF) leg featured an actuated hip and knee, and an unactuated, compliant foot joint. Other work on dynamic quadrupeds includes Raibert's most recent foray into legged robots using similar design and control ideas as found in Scout II: the bounding AIBO, [15].

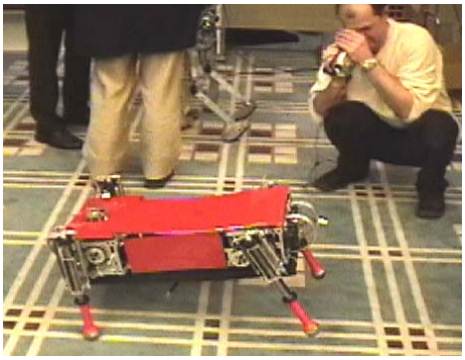

Figure 1. Scout II: A high performance, autonomous four-legged robot, running during a demonstration in Kyoto, Japan.

Various models have been proposed to study dynamically stable quadrupeds. Murphy and Raibert studied bounding and pronking using a model with kneed legs whose lengths were controllable, [8]. They discovered that active attitude control in bounding is not necessary when the torso's moment of inertia is smaller than the mass multiplied by the square of half the hip spacing. Following up on their work, Berkemeier used a simple linearized running-in-place model and concluded that Murphy's result is valid and can be extended in pronking when particular inequalities are satisfied, [1]. More recently, Poulakakis et al. showed that passively generated stable bounding of a conservative model of Scout II is possible under appropriate initial conditions, [10]. In a different spirit, Formalsky et al. investigated ballistic motions of a quadruped model that were achieved by appropriate initial speeds resulting from impulsive active control torques, [2]. Although, many models for open or closed loop dynamic legged locomotion have been extensively studied, e.g. [1], [2], [8], [13], and many simulation techniques have been proposed for efficient integration of the dynamic equations, e.g. [3], *no* models which are experimentally validated down to the actuator torque level by physical prototype robots exist in the

[1] Work performed while Assoc. Professor at McGill University.

literature. Addressing this issue constitutes the central contribution of this paper.

In this paper, the authors attempt to assess the viability of various simplifying assumptions usually made in the literature for deriving models suitable for analyzing dynamic legged locomotion. Rather than concentrating on the analytical derivation and efficient integration of the equations of motion, we turn our attention into testing various modeling assumptions. This is done by constructing two simulation models exhibiting different levels of modeling complexity, towards determining which assumptions are reasonable for Scout II. Similar features are also likely to be important in other dynamic robots. Comparison of simulation results with a large number of experimental data showed remarkable accuracy, considering the complexity of the system.

II. Scout II Bounding

In this paper, we restrict our attention to the bounding running gait, in which the essentials of the motion take place in the sagittal plane. Therefore, Scout II can be considered as a three-body kinematic chain, see Fig. 2, composed of the torso and the front and back virtual legs. Since each of the two legs can be in stance or flight, there are four *robot states*: double leg flight, double leg stance, back leg stance and front leg stance.

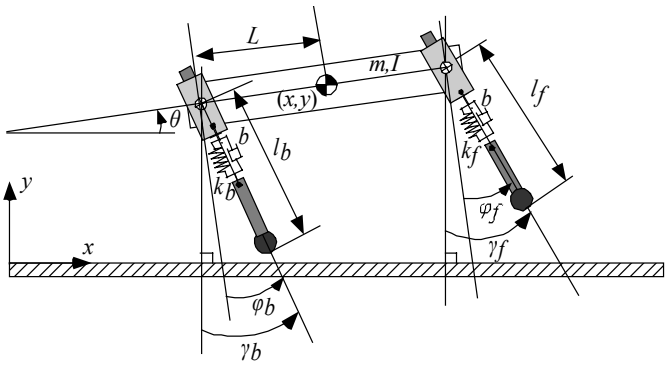

Figure 2. Sagittal plane model for Scout II.

In each of these phases, the equations of motion are different. The two-dimensional model presented in Fig. 2, can be described by seven coordinates,

$$\mathbf{x} = \begin{bmatrix} x & y & \theta & \varphi_b & l_b & \varphi_f & l_f \end{bmatrix}^T . \qquad (1)$$

A. Preliminary Bounding Controllers

Scout II is an underactuated, nonlinear, intermittent dynamical system, whose task cannot be encoded in terms of some desired trajectories. But even if such trajectories could be found, developing a tracking controller is still not straightforward. Friction, actuator limitations and unilateral ground forces limit the hip torques, which may be required to achieve trajectory tracking. Furthermore, there are no experimentally validated models for legged robots, which could be used to derive model-based controllers. This reveals the necessity of constructing simulation models to test the validity of various simplifying modeling assumptions, which constitutes a central issue of this paper and will be discussed in Section IV.

Despite this complexity, the authors found that simple, Raibert-style controllers operating mostly in a feedforward fashion, with minimal sensing, result in robust and fast running, powered by only the four hip actuators, [9], [14].

The leg pairs detect three possible *leg states*: stance-retraction, stance-brake and flight, which are separated by touchdown, sweep limit and lift-off events, see Fig. 3. Depending on these states, different control actions are assigned by the high-level controller (Fig. 4).

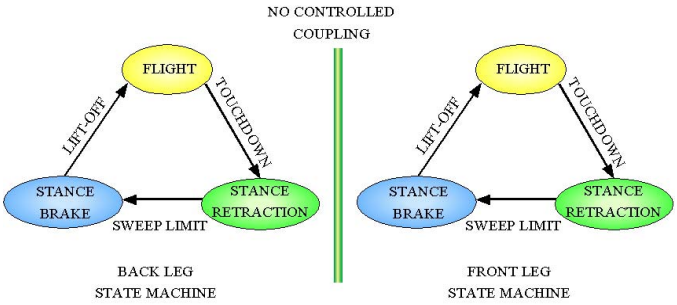

Figure 3. The bounding controller state machine.

Flight. During the flight leg state, the controller servos the leg to a desired touchdown angle. This desired angle is defined with respect to the body and is fixed throughout flight.

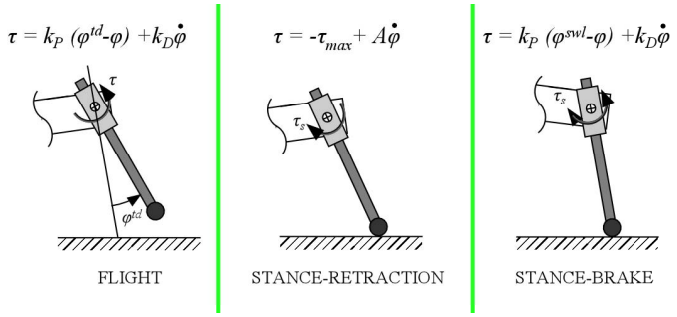

Figure 4. Control action for each leg state in the bounding gait.

Stance-retraction. During this leg state, the controller sweeps the leg backwards, until the sweep limit event is reached. In this phase, actuators typically operate at their limits, characterized by their torque-speed curve. While this curve is well known, it is rarely taken into account in robot modeling and control, [14]. To include motor saturation into the controller, torques are commanded according to the prescription

$$\tau_{\text{des}} = -\tau_{\max} + A\dot{\varphi}\,, \qquad (2)$$

$$\tau_{\max} = \frac{K_T \bar{V}}{R_A}\,,\quad A = -\frac{K_T K_\omega}{R_A}\,, \qquad (3)$$

where $\tau_{\max}$, A are the offset and the slope of the torque speed line, K_T, K_ω are the torque and speed constants of the Maxon 118777 motor and R_A is its armature resistance, [7]. In (3), $\bar{V}$ is the average voltage at the motor terminals, which is set to 36 V. Note that there are two additional constraints that must be imposed on the commanded torques, i.e.

$$\text{if } |\tau_{des}| > K_T\, i_{\max} \text{ then } \tau_{des} = -K_T\, i_{\max}\,, \qquad (4)$$

$$\text{if } \tau_{des} \geq 0 \text{ then } \tau_{des} = 0\,. \qquad (5)$$

The constraint (4) ensures that the commanded torque will not exceed the maximum predicted by the amplifier current limit $i_{\max}$. The constraint (5) prevents the commanded torque from becoming positive, thus decelerating the robot[2].

Stance-brake. When the sweep limit event is reached i.e. when the leg angle becomes smaller than a specific sweep limit angle (a controller parameter) a PD controller servos the leg at that angle. Although this modification has the undesirable effect of braking the robot, it is necessary for ensuring toe clearance in the protraction phase, because of the absence of active control of the leg length during flight.

B. The Bounding Gait

Fig. 5 presents snapshots of Scout II along with experimental data showing the cyclicity of the motion during a bounding run. The controller parameters used for each of the physical legs are presented in Table I and the resulting average forward speed was approximately 1.3 m/s. Based on the above control strategy a family of controllers was introduced by changing the control action during flight or stance, [14]. It is remarkable that the significant controller differences have relatively minor effects on bounding performance. Moreover, variations on this controller recently resulted in the half-bound and rotary gallop gaits for the first time, [11].

TABLE I
CONTROLLER PARAMETERS (SI UNITS, ANGLES IN DEGREES)

Parameter	Front	Back
Touchdown Angle	21	19
Sweep Limit Angle	0	0
Flight (k_P, k_D)	(250, 5)	(250, 5)
Stance-brake (k_P, k_D)	(300, 5)	(300, 5)

III. MODELING COMPONENTS

Through the course of this research it has became clear that modeling only the motor driving system (batteries, PWM amplifiers and actuators), as in [14], is *not* sufficient for obtaining simulation results which closely follow the experimental data. A more detailed model of the hip unit, which includes backlash and belt compliance, must be included in simulation in order to improve the accuracy of the simulation results. The assumptions of zero backlash and rigid torque transmission are very common in modeling dynamically stable robots, despite the presence of gearboxes and belts in leg designs. As will be shown in Section IV, for Scout II and the controllers presented in Section II, these assumptions result in mismatches between simulation and experimental data.

To capture these effects, the three stage planetary gearbox has been approximated by a pair of spur gears as in Fig. 6, with gear ratio equal to the combined gear ratios of the gearbox and pulleys. In addition, friction and damping present in the hip joint were taken into account to improve the leg response during the flight phase. To estimate the values of the inertias of the drive and driven gears and the friction and damping coefficients of the hip joint, two sets of experiments were performed. In the first set a known mass was placed at the toe, the leg was brought to a known angle and then it was left to rotate freely. In the second set, the robot was placed so that both the front and back legs were in flight and various touchdown angles were commanded. All these experiments were simulated in Working Model 2D™, [6], and the resulting parameter values are presented in Table II for the physical legs.

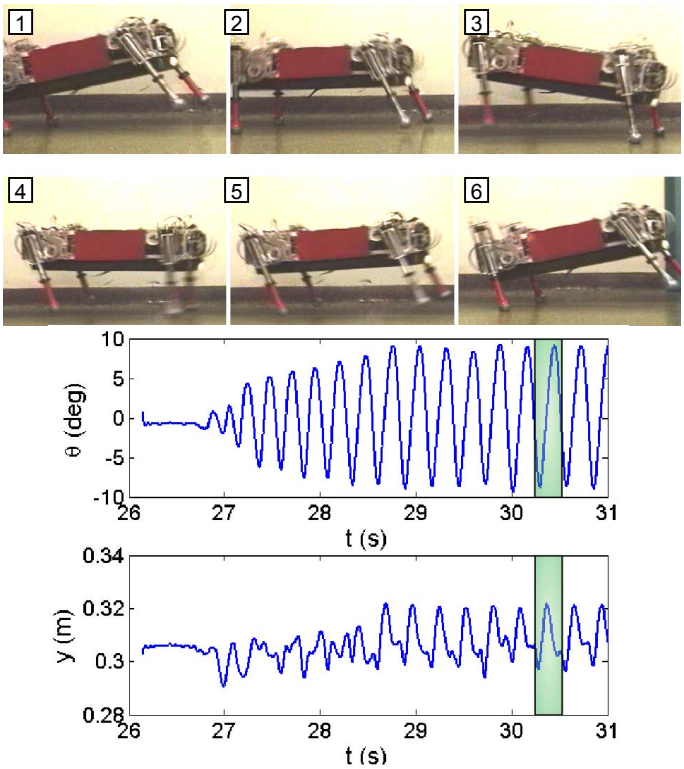

Figure 5. Snapshots of the robot at different phases (upper) and pitch angle and hopping height plots (lower) during one experimental run. The shadowed window corresponds to the stride studied in detail in Section IV.

Finally, the combined effect of gear backlash and belt compliance has been approximated by a rotational spring in parallel with a damper as shown in Fig. 6. The values of the hip spring/damper constants were chosen so that the maximum spring deflection during bounding in simulation does not exceed that which is measured by the robot applying maximum hip torque with the torso and legs constrained on a horizontal plane (approximately 8°).

In all the above experiments, none of the structural elements was examined in isolation. For instance, isolating the gearbox and performing detailed identification experiments to find the inertia of the gears requires special equipment not available to the authors, and even if such data were available finding the "equivalent" inertias of the spur gears used in this model is far from trivial. Instead, we decided to perform simple experiments examining the behavior of the hip unit as a whole under different dynamic conditions as described above. Then parameter values were selected that resulted in better match between experiment and simulation under all these different conditions. Note that exact fitting of simulation results to experimental data was

[2] (4) arises when $\dot{\varphi}$ is too small so that excessively large torques are predicted from (2). (5) occurs when the legs are spinning at speeds large enough to result in a change of sign of the commanded torque.

impossible. Therefore, the values were chosen via trial and error by comparing simulation and experimental data.

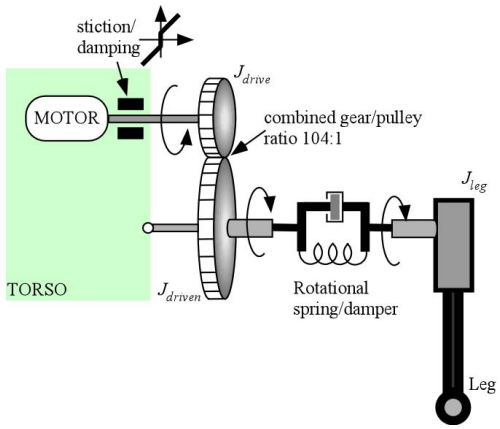

Figure 6. Details of the hip unit model.

TABLE II
HIP JOINT PROPERTIES

Parameter	Value	Units
Drive Gear Inertia	$3.5\ 10^{-6}$	kg m^2
Driven Gear Inertia	10^{-3}	kg m^2
Stiction (joint)	$5.5\ 10^{-3}$	Nm
Damping (joint)	$6.2\ 10^{-7}$	Nm/deg/s
Spring (belt)	7.0	Nm/deg
Damper (belt)	4.0	Nm/deg/s

IV. EXPERIMENTS AND SIMULATIONS

At this point one must mention that simulating the open-loop intermittent dynamics of a mechatronic system that exhibits various constraints and interacts with its environment, like Scout II, is a very challenging task. The absence of strong feedback control, which would "push" the dynamics towards some *a priori* known desired trajectories, the errors associated with the identification experiments, the uncertainty in the knowledge of some parameters provided by manufacturers of certain components e.g. dynamic gearbox efficiency, in combination with the intermittent nature of the system, are some of the qualities which make the task of obtaining an accurate simulation model far from being trivial. In this section the two models used to simulate bounding are presented and then a comparison between experiment and simulation is made. To generalize the conclusions statistical data for a large number of bounding strides are presented.

A. Simulation Models

The planar model of Scout II, see Fig. 7, was constructed in Working Model 2D™ to study the behavior of the robot under various controllers. The animation step is set to 1 ms, which is the control loop time step used in the robot. To obtain the simulation results, the adaptive step Kutta-Merson integrator was used with integration error set to 1e-10.

In the simplest simulation model, called *Model I*, see Fig. 7a, the legs are attached to the torso via an actuator constraint, which applies torques to the leg taking into account the actuator limitations. In the full model, called *Model II*, see Fig. 7b, the hip unit has been modeled in more detail as shown in Section III. The leg is attached to the driven gear via a rotational spring/damper system and the driven gear is attached to the drive gear via a gear constraint implementing the combined gear ratio of the gearbox/sprocket. The values of the design parameters are presented in Table III.

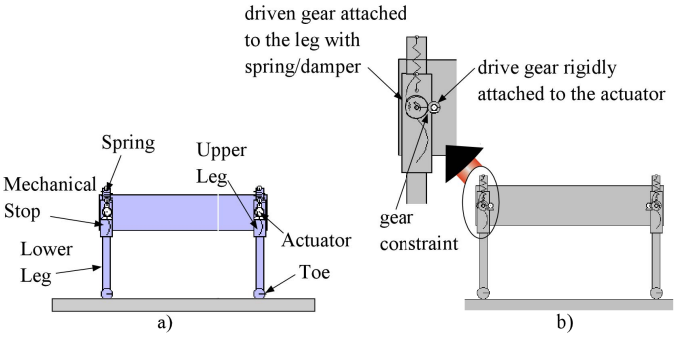

Figure 7. Scout II planar model built in Working Mode 2D™: (a) Model I and (b) Model II.

TABLE III
BASIC MECHANICAL PROPERTIES OF SCOUT II

Parameter	Value	Units
Torso Mass	20.865	kg
Torso Inertia	1.3	kg m^2
Leg Mass	0.97	kg
Leg Inertia	0.01	kg
Spring Constant	3520	N/m
Damping Constant	55	N/m/s
Hip Spacing	0.552	m
Leg Length	0.323	m
Sprocket Combination	48/34	n/a
Sprocket Efficiency	96%	n/a
Planetary Gear Ratio	72.38	n/a
Max. Gear Efficiency	68%	n/a

B. Simulation and Experimental Results

In this section the comparison between simulation and experimental data is undertaken. The controller gains and set points in simulation are exactly the same as those used in experiment and presented in Table I. For the sake of clarity the torso state variables are presented in detail for one stride while the leg variables are presented for one step.

Fig. 8 shows the pitch angle and hopping height in experiment and in both simulation models, corresponding to the highlighted region in Fig. 5. In experiment, the pitch and center of mass (COM) height are measured using two laser range finders located at the front and back ends of the torso. The laser data were low-pass filtered at 15 Hz after-the-fact via FFT analysis in Matlab™. Unfortunately, as can be seen from Fig. 8, the remarkable match in the pitch angle did not extend to the COM height where the difference between simulation and experiment, especially in *Model I*, is significant. This is attributed to the stiction and nonlinear damping (depends on the leg angle and applied torque) effects which are inherent in the telescopic leg design and are not included in the simulation model. The difference in shape results from the dependence of the COM hopping height on both translation and rotation of the torso, which are coupled to the leg state sequence; in experiment front leg touchdown occurs slightly after back leg lift-off while in simulation it occurs slightly before.

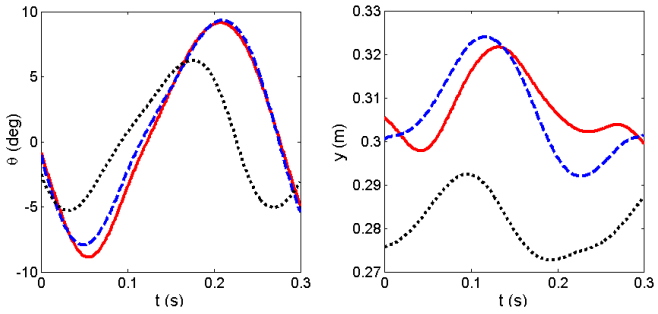

Figure 8. Steady state pitch angle (left) and hopping height (right) during one stride. Experiment (solid), Model I (dotted) and Model II (dashed).

Fig. 9 shows the angles and angular velocities of the front and back legs relative to the torso. For clarity, back and front leg plots correspond to one step and are synchronized based on the corresponding lift-off events. As expected, the leg response during the flight phase is significantly improved in *Model II*. In the retraction-stance and brake-stance phases of both virtual legs the discrepancy between experimental and simulation results is larger, as expected. The main source of errors in both models is the simplifying assumptions in modeling the hip joint. However, including the hip model described in Section III significantly improves the accuracy of the simulation during the stance-brake phase. This is evident especially in the back legs where, in *Model I*, the sweep limit controller is not able to hold the leg at the desired sweep limit angle. This effect significantly affects the simulation results to the point where cyclic motion might not even be achievable with the set points and gains used in experiment, as in [14].

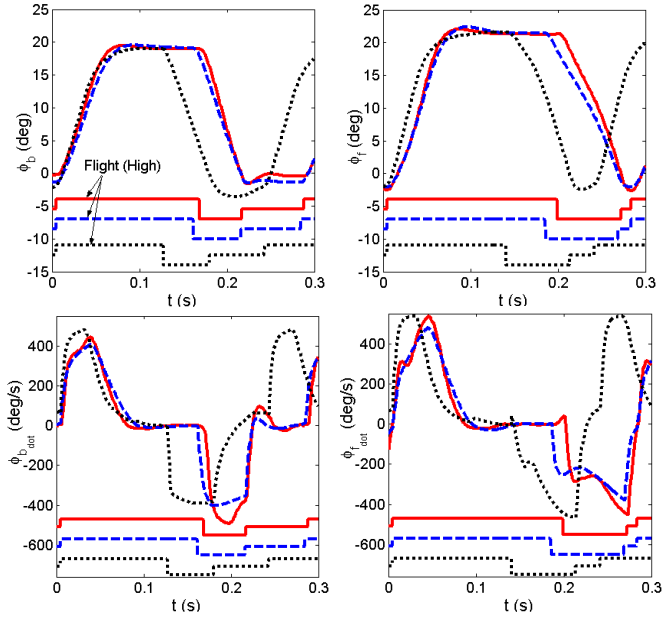

Figure 9. Back (left) and front (right) leg angles (upper) and leg angular velocities (lower) during one step. Experimental data (solid), Model I (dotted) and Model II (dashed). The square wave represents the leg states: Flight (high), stance-retraction (low) and stance-brake (medium).

The stance-brake phase is very difficult to model because it depends on the interaction of several effects, which are difficult to estimate. In experiment, when the sweep limit is reached the motor initially loads the torsional leg-belt-gear compliance without actually *feeling* the full load of the robot. Then, depending on ground friction *and* lift-off time instant (that depends on the robot's state) slipping might be present or contact with the ground might be lost. Thus, in experiment, it is *easier* for the motor to hold the leg at the desired angle than in *Model I*, a fact captured by *Model II*.

Fig. 10 presents the torques applied by the motors in experiment and simulation. As expected there are relatively large discrepancies between the torques predicted by *Model I* and the torques estimated in experiment. These differences are coupled to those observed in the leg angle rates, since motor saturation and thus torque application depends significantly on the leg speed. In *Model II* the simulation predicted torques are much closer to the current-estimated torques in experiment. However, there are still some issues that need to be resolved to provide a better match. For instance, the gearbox efficiency varies as a function of the applied torque. In all the simulations the maximum gearbox efficiency, a constant, was used to command and estimate torques. However, the gearbox efficiency drops dramatically when the applied torque is small, a fact that might explain discrepancies between *Model II* and experiment (which are more intense when the torque is small). Maxon describes how the efficiency of the gearbox changes with the applied torque. Unfortunately, this information is only qualitative and thus it has not been used in the simulation results presented here.

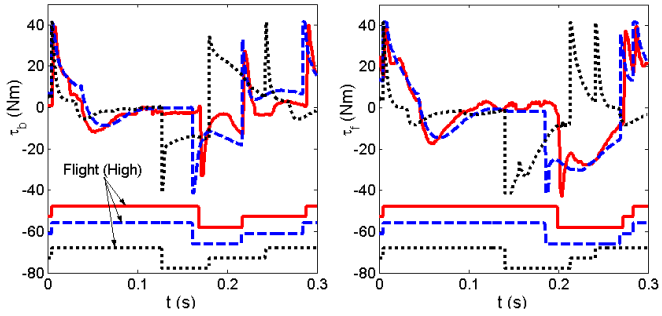

Figure 10. Back (left) and front (right) leg torques during one step. Experimental data (solid), Model I (dotted) and Model II (dashed). The square wave represents the leg states: Flight (high), stance-retraction (low) and stance-brake (medium).

Fig. 11 shows the leg angular speed as function of the applied motor torque in experiment and simulation. One can see that the motors are saturated most of the time and that both simulation models adequately capture this effect.

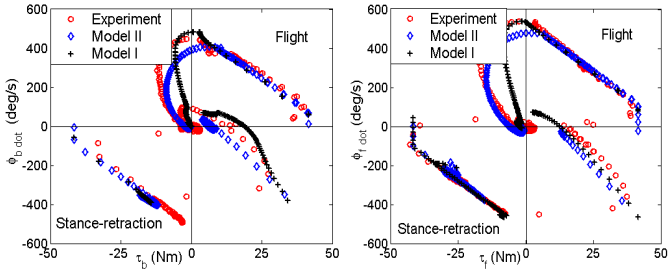

Figure 11. Back (left) and front (right) motor saturation characteristics.

It is apparent from Fig. 11 why motor characteristics must be taken into account. Careful inspection of Fig. 11 reveals that most of the discrepancies lie in the nonsaturation region,

where the applied torques mostly depend on the dynamics of the system. Note also, according to the sign conventions shown in Fig. 2, that during stance-retraction the motors operate in the third quadrant while during flight they operate in the first quadrant (positive torques correspond to the leg moving forward).

C. Simulation Error Assessment

In this section an attempt is made to assess the quality of the simulation results obtained using the simulation models described above. To do so, the results presented above for one stride have been generalized to multiple strides corresponding to different bounding experiments. Thus, for the comparison ten bounding experiments were performed on carpet, in each of which the robot took at least seven steady state strides defined by the back leg lift-off event. The existence of phase difference between simulation and experimental results precludes calculation of errors of the state variables in time (e.g. comparing L_2 norms). Therefore, the comparison is undertaken in terms of percent errors in some key gait parameters i.e. stride frequency ω_s, duty factor β, and the max and min values of the torso's pitch angle and hopping height over the 70 strides taken, as reported in Fig. 12.

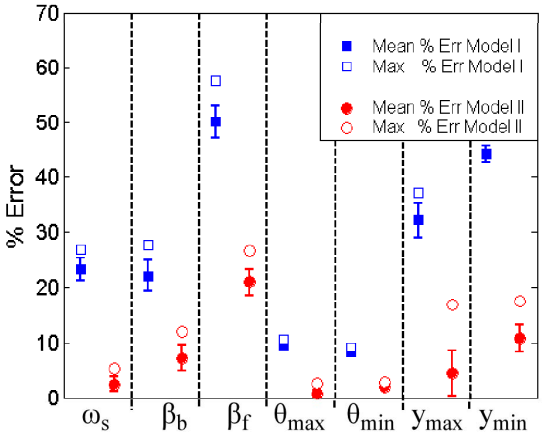

Figure 12. Mean and max errors between simulation models and experimental results in stride frequency, leg duty factors and max and min values of the pitch angle and hopping height over 70 bounding strides. The average forward speed was 1.3 m/s approximately.

Note that apart from the inaccuracies discussed in Section IV B, another source of error is the deviation of the robot from the sagittal plane during some of the experiments. However, despite the simplifying assumptions and the uncertainty associated with some of the design parameters, it can be seen that *Model II* captures the behavior of the robot not only qualitatively. Indeed, the average errors for *Model II* in all the parameters are below the corresponding ones for *Model I*, and most strikingly, all are smaller than 25%, which is very good for dynamically stable robots.

V. Conclusion

In this paper the authors presented an algorithm that controls compliant bounding for a quadrupedal robot with only one actuator per leg. Two different simulation models were constructed to test the validity of commonly made assumptions in modeling dynamic legged robots. Both models included an experimentally validated motor driving system with battery model; without the actuator saturation taken into account the models do not converge to cyclic motion. To construct a model that accurately describes the physical robot one needs to include a detailed model of the hip joint including torsional belt compliance and gear dynamics; the assumption of rigid torque transmission is not valid and significantly affects the accuracy of the results. The resulting model is remarkably accurate despite the complexity of Scout II. The authors hope that these results will shed light into which commonly made assumptions (e.g. constant max torque, rigid torque transmission) might result in misleading models. Including these assumptions will lead to simulations that will allow developing controllers with fewer tiresome trial and error experiments with the robot.

Acknowledgment

The work of I. Poulakakis has been supported by a R. Tomlinson Doctoral Fellowship and a Greville Smith McGill Major Scholarship.

References

[1] Berkemeier M. D., "Modeling the Dynamics of Quadrupedal Running," *Int. J. of Robotics Research*, Vol. 17, No 9, pp. 971 – 985, 1998.

[2] Formalsky A., Chevallereau C. and Perrin B., "On Ballistic Walking Locomotion of a Quadruped," *Int. J. of Robotics Research*, Vol. 19, No. 8, pp. 743-761, 2000.

[3] Freeman P. S. and Orin D. E., "Efficient Dynamic Simulation of a Quadruped Using a Decoupled Tree-Structure Approach," *Int. J. of Robotics Research*, Vol. 10, No. 6, pp. 619-627, 1991.

[4] Furusho J., Sano A., Sakaguchi M. and Koizumi E., "Realization of Bounce Gait in a Quadruped Robot with Articular-Joint-Type Legs," *Proc. of the IEEE Int. Conf. on Robotics and Automation*, pp. 697-702, 1995.

[5] Kimura H., Akiyama S. and Sakurama K., "Realization of Dynamic Walking and Running of the Quadruped Using Neural Oscillator," *Autonomous Robots*, Vol.7, No.3, pp. 247-258, 1999.

[6] Knowledge Revolution, *Working Model 2D User's Guide*, Ver. 5.0, San Mateo, CA, 1996. http://www.krev.com/.

[7] Maxon Motors AG, *Motor Product Catalog*, p.77, 1997.

[8] Murphy K. N. and Raibert M. H., "Trotting and Bounding in a Simple Planar Model," *Tech. Rep. CMU-LL-4-1985*, Carnegie Mellon University, The Robotics Institute, pp. 57-88, 1985.

[9] Papadopoulos D. and Buehler M., "Stable Running in a Quadruped Robot with Compliant Legs," *Proc. of the IEEE Int. Conf. on Robotics and Automation*, pp. 444 – 449, 2000.

[10] Poulakakis I., Papadopoulos E. and Buehler M., "On the Stable Passive Dynamics of Quadrupedal Running," *Proc. of the IEEE Int. Conf. on Robotics and Automation*, 2003.

[11] Poulakakis I., Smith J., and Buehler M., "On the Dynamics of Bounding and Extensions Towards the Half-Bound and the Gallop Gaits," *Int. S. on Adaptive Motion of Animals and Machines*, 2003.

[12] Raibert M. H., *Legged Robots that Balance*, MIT Press, Cambridge MA, 1986.

[13] Schmiedeler J. P. and Waldron K. J., "The Mechanics of Quadrupedal Galloping and the Future of Legged Vehicles," *Int. J. of Robotics Research*, Vol. 18, No. 12, pp. 1224-1234, 1999.

[14] Talebi S., Poulakakis I., Papadopoulos E. and Buehler M., "Quadruped Robot Running with a Bounding Gait," *Int. S. Experimental Robotics VII*, pp. 281-289, 2001.

[15] Yamamoto Y., Fujita M., De Lasa M., Talebi S., Jewell D., Playter R. and Raibert M., "Development of Dynamic Locomotion for the Entertainment Robot – Teaching a New Dog Old Tricks," *4th Int. Conf. on Climbing and Walking Robots*, pp. 695 - 702, 2001.